Experimental Study on Ratcheting of Cylinder Subjected to Axially Moving Temperature Distribution

Toshihide Igari, Masafumi Yamauchi
Mitsubishi Heavy Industries, Ltd., Nagasaki, Japan
Yoshio Kamishima
Mitsubishi Atomic Power Industries, Ltd., Tokyo, Japan
Hiroshi Wada
Mitsubishi Heavy Industries, Ltd., Kobe, Japan

OBJECTIVE

Prevention of progressive deformation by plastic ratcheting is one of the concerns in the design of high temperature components in fast breeder reactors. The ratcheting under the combination of primary and secondary stresses(Bree, 1968, Roche et al. 1982) is considered in the design codes, on the other hand, ratcheting phenomena under the secondary stress alone have been paid attention(Gokhfeld et al., 1980), such as a ratcheting of cylinder subjected to axially moving temperature distribution. Development of a design criterion for this ratcheting is very important in the design of the reactor vessel of fast breeder reactor containing high-temperature sodium. So far, however, a mechanism and a prediction method for this ratcheting have not been clarified. In the related paper(Wada et al., 1989), the authors proposed the ratcheting mechanism as well as the predictive equations of the ratcheting strain for the representative two temperature distributions. The proposed ratcheting mechanism was based on the hoop-membrane stress-strain behavior of the cylinder, and the movement of the temperature distribution was regarded as a driving force of this ratcheting. This paper describes the results of the experimental study on the proposed ratcheting mechanism and the predictive equations.

OUTLINE OF THE PROPOSED MECHANISM AND PREDICTIVE EQUATIONS

The authors proposed the hoop-membrane-stress-based ratcheting mechanism for a cylinder subjected to the axial movement of the representative temperature distribution as shown in Fig.1. According to this mechanism, the movement of the temperature distribution is a driving force of this ratcheting. That is to say, the ratcheting occurs in the hot or cold front cycling, on the other hand, the ratcheting does not occur in the stationary cycling in which the temperature distribution does not move. As for the moving directions of the temperature distribution, an expanding ratcheting in the cold front cycling and an shrinking ratcheting in the hot front cycling occur for the case of the step change. On the other hand, expanding ratcheting occurs independent of the moving direction for the case of the linear change with a folding at the low temperature. And the shrinking ratcheting occurs independent of the moving direction for the case of the linear change with a folding at high temperature. The predictive equations for the ratcheting strain are proposed as follows for the two temperature distributions, by assuming an elastic- perfectly-plastic material neglecting the dependence of material constants on temperature,

$$\varepsilon_\theta^R=(\Delta\sigma_{\theta,el}-2\sigma_y)/E=2(\sigma_{\theta,el}-\sigma_y)/E \qquad \text{(Step change)} \qquad (1)$$

$$\varepsilon_\theta^R=2(\sigma_{\theta,el}-\sigma_y)/E \qquad \text{(Linear change)} \qquad (2),$$

where ε_θ^R, $\Delta\sigma_{\theta,el}$, $\sigma_{\theta,el}$, σ_y and E are the ratcheting strain per one cycle, the range of elastically-calculated-hoop-membrane stress, the elastically-calculated-maximum-hoop-membrane stress, yield stress, and Young's modulus, respectively.

EXPERIMENTAL APPARATUS

The general view of the experimental apparatus is schematically shown in Fig.2. The test specimen with a shape of a hollow cylinder with an outer diameter of 140mm, a thickness of 1mm is attached to a fatigue-testing machine by using the expansion joint. The test specimen is made from a pipe (JIS SUS304TP) with an outer diameter of 165.2mm and a thickness of 18.2mm. Mechanical properties of the test material are listed in Table 1. Cooling water is filled in the test specimen, and the water level is kept constant. By the combination of this cooling water and the high-frequency-induction-heating coil surrounding the test specimen, axially-distributed-axisymmetric temperature distribution with a maximum temperature of 650°C and a maximum temperature gradient $\Delta T/\Delta Z$ of 75°C/mm is generated. The temperature distribution was measured at both inner and outer surfaces of the cylinder. The temperature difference between the inner and the outer surfaces is small enough. Since the height of both the water level and the induction-heating coil is fixed, the temperature distribution moves up and down against the test specimen when the test specimen moves slowly by using the fatigue-testing machine.

CONDITION OF EXPERIMENT

The experimentally-obtained temperature distribution at the center of thickness with the maximum temperature of 650°C and the axial-temperature gradient of 75°C/mm is shown in Fig.3 together with the elastically-calculated axial and hoop stresses at the outer surface, the center of thickness and the inner surface. The analytical results were obtained by using the axisymmetric shell element of ABAQUS code and by considering the temperature dependence of material constants. The elastic stress intensity $S_n(=\Delta|(\sigma_z-\sigma_\theta)|)$ at the outer surface is equal to 1037MPa, and the maximum and the minimum hoop membrane stresses are 299MPa(at 125°C) and -186MPa(at 550°C) respectively. The maximum and the minimum hoop membrane stresses exceed the 0.2% yield stress at the 125°C and 550°C respectively, and so the plastic deformation does occur at both portions of the maximum and the minimum stresses. These two portions are close enough to each other, when compared with π/β $[\beta=\{3(1-\nu^2)/r^2t^2\}^{1/4}]$, and so the ratcheting mechanism for the case of the step change can be examined by using this temperature distribution. The following three cases of experiment were performed.

Case 1: Stationary cycling of the temperature distribution
Case 2: Hot front cycling of the temperature distribution
Case 4: Cold front cycling of the temperature distribution

In the hot and cold front cyclings, the temperature distribution is loaded up to the steady temperature profile with the maximum temperature, and is moved 60mm with a moving speed of 6mm/min, and finally is unloaded until the test specimen reaches the room temperature. This condition is cycled up to the maximum cycles of 100. The test condition is shown in Table 2 together with the elastic stress for each temperature distribution. The elastic stress intensity of these three cases is about the same to each other. The auxiliary three cases for studying the effect of stress level and moving distance are also examined as shown in Table 2.

RESULTS

The residual deformation at 100th cycle for the stationary cycling(Case 1) is shown in Fig.4 together with the respective temperature distribution. The residual deformation for the case of the hot and the cold front cycling(Case 2 and Case 4) is shown in Figs.5 and 6 respectively. The progress of ratcheting strain $\varepsilon\theta^R(=\delta/r_{mean})$ is shown in Fig.7 for these three cases. As for the Case 1, little ratcheting occurs after 100 cycles, on the other hand, both Case 2 and Case 4 with a movement of temperature distribution show a remarkable ratcheting, and the expanding ratcheting and shrinking ratcheting occur for the cold front cycling and the hot front one respectively. The ratcheting strain after 50 cycles is shown in Fig.8 against the stress intensity Sn. In this figure, all data except for the case 1 are included, and as the stress level grows larger, the ratcheting strain shows a larger value. By comparing the results of Case 4 and Case 5, the reduction of the ratcheting strain can be seen when the moving distance is reduced.

DISCUSSION

The ratcheting mechanism proposed in the related paper(Wada et al, 1989) was verified by comparing the ratcheting behavior of the stationary cycling and that of the hot/cold front cyclings. The difference between the ratcheting behavior of the hot front cycling and that of the cold front cycling also supports the proposed ratcheting mechanism. The ratcheting behavior of Case 3 where the hoop membrane stress in only the cold side exceeds the yield stress showed an expanding in the hot front cycling as shown in Fig.8. This case can be understood by considering the ratcheting mechanism for the linear change.

Before making use of the proposed predictive equation for the experimental results, the dependence of yield stress on temperature in eqs.(1) and(2) must be examined. As for the case of the linear change, it seems plausible to use the yield stress at the folding point of the temperature distribution. As for the case of the step change, a study is necessary by considering the moving direction and the two kinds of yield stress at the hot and cold temperatures, σ_{yH} and σ_{yC}. Just as supposed from the assumption in the related paper(Wada et al., 1989), the hoop-membrane stress-strain hysteresis loop for the case of the hot front and the cold front will have a shape as shown in Fig.9. That is to say, in the case of the hot front, plastic deformation does not occur at B, and the yield stress in eq.(1) is considered to be σ_{yH}. In the case of the cold front, on the other hand, plastic deformation occurs in the process from A to B. Since the amount of the plastic strain in the process from A to B is undetermined, the ratcheting strain in the cold front is conservatively predictable by using σ_{yC} as the yield stress in the eq.(1). The assumption of the stress-strain behavior in Fig.9 is consistent with that suggested by Goodman(Goodman, 1978).

Prediction was made for Cases 2, 3, 4 and 6, where the length of moving is long enough. The predictive equations for cases 2, 3, 4, and 6 are as follows.

$$|\varepsilon\theta^R|=2(|\sigma\theta,_{el}|-\sigma_{yH})/E \qquad \text{Case 2} \qquad (3)$$

$$\varepsilon\theta^R=2(\sigma\theta,_{el}-\sigma_{yC})/E \qquad \text{Cases 3, 4, 6} \qquad (4)$$

In the Case 2, the minimum hoop membrane stress by elastic analysis was taken as $\sigma\theta,_{el}$, and in other cases the maximum hoop membrane stress is taken as $\sigma\theta,_{el}$. Since the hoop membrane stress in the hot side was below σ_{yH}, the case 3 was regarded as the linear change. As values of σ_{yH} and σ_{yC}, 0.2% yield stresses at 550°C and 125°C, that is to say, 142MPa and 215MPa, were adopted respectively.

In order to discuss all these cases in a unified manner, the non-dimensional expression in the following form was adopted.

$$\varepsilon\theta^R/(\sigma_y/E)=2(\sigma\theta,_{el}/\sigma_y-1) \qquad (5)$$

Figure 10 shows results of prediction for both the ratcheting strain increment per one cycle and the accumulated ratcheting strain at 50th cycle. Experimental data were also shown in the figure for both the averaged ratcheting strain increment in the initial 3 cycles and the accumulated ratcheting strain at 50th cycle. As for the ratcheting strain increment, good prediction was made for most of the cases, and the case 4 showed a larger value than prediction. Prediction at the 50th cycle gave conservative results because the work hardening and/or cyclic hardening were involved in the experimental results.

The experimental conditions are not categorized exactly to the step change or the linear change, but it is found that the quantitative prediction by the proposed equations is possible to some extent. And it is found that the conservative prediction is possible at the large number of cycles.

CONCLUSION

Experimental study was made on a hollow cylinder subjected to axially moving temperature distribution. Obtained results are as follows:

(1) Little ratcheting occurs for the stationary cycling, on the other hand, the remarkable ratcheting does occur for the cold and hot front cycling. The inverse ratcheting behavior occurs in the cold and hot front cycling. These behavior verified the proposed ratcheting mechanism.

(2) The predicted results for the ratcheting strain at initial cycles comparatively coincided with the experimental results.
And the conservative prediction was possible at the large number of cycles where the work hardening and/or cyclic hardening were involved in the experiment.

REFERENCES

Bree,J. (1968), J.Strain Analysis, Vol.3 P122

Gokhfeld,D.A. and Cherniavsky,O.F. (1980), Limit Analysis of Structures at Thermal Cycling, P450, Sijthoff & Noordhoff

Goodman,A.M., Non-linear problems in stress analysis, Stanley,P. Ed., Applied Science Publishers, P317

Karadeniz,S., Ponter,A.R.S and Carter,K.F. (1987), J.Pressure Vessel Technology, Vol.109, P387

Roche,R.L., Moulin,D. and Lebey,J. (1982), Nuclear Engineering and Design, Vol.71, P51

Wada,H., Igari,T. and Kitade,S. (1988), Trans. SMiRT-10 Div.L

Table 1 Mechanical properties of test material

Temp. (°C)	0.2% yield stress (MPa)	Tensile strength (MPa)	Elongation (%)	Reduction of area (%)
RT	258	592	69.5	81.8
650	134	310	46.4	77.6

Table 2 Condition of experiment

Case No.	Tmax (°C)	Loading pattern	l(mm) (βl)	Sn (MPa)	$\sigma_{\theta C}$ (MPa)	$\sigma_{\theta H}$ (MPa)	Maximum cycle Nmax
1	650	Stationary	0	1037	299	-186	100
2		Hot front	60 (5.60)	1053	321	-195	
3				786	246	-95	
4		Cold front		1002	288	-181	50
5			10(0.93)	1031	292	-205	100
6	550		60(5.60)	844	263	-143	

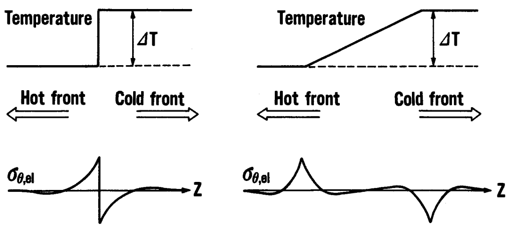

(a) Step change (b) Linear change

Fig.1 Representative temperature distributions

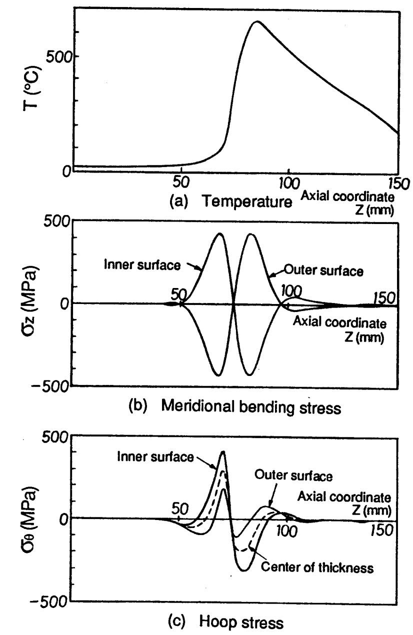

(a) Temperature (b) Meridional bending stress (c) Hoop stress

Fig.3 Elastic stress distribution (Case 1)

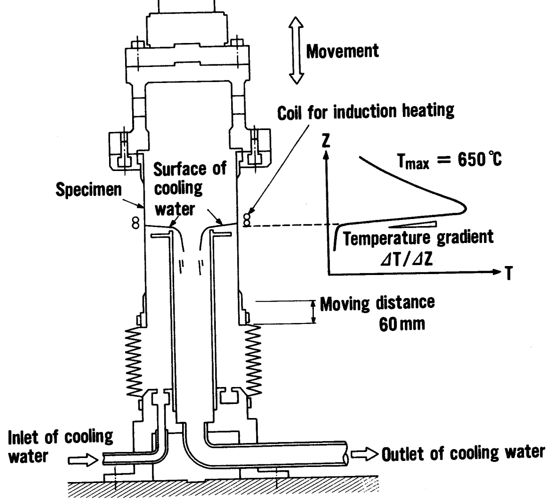

Fig.2 General view of testing apparatus

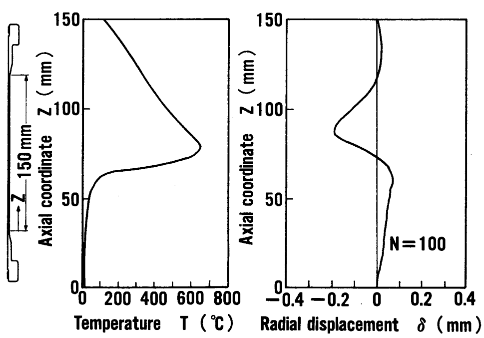

Fig.4 Residual deformation (Case 1)

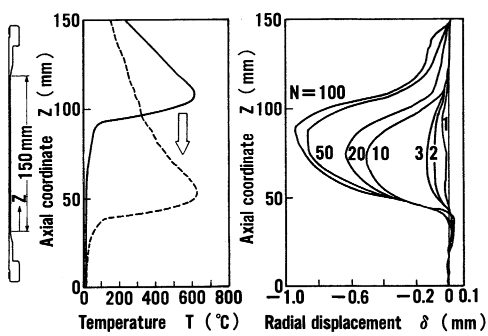

Fig.5 Residual deformation (Case 2)

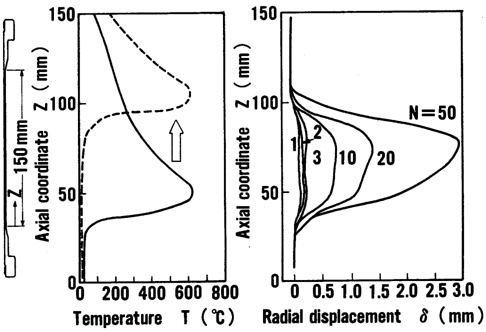

Fig.6 Residual deformation (Case 4)

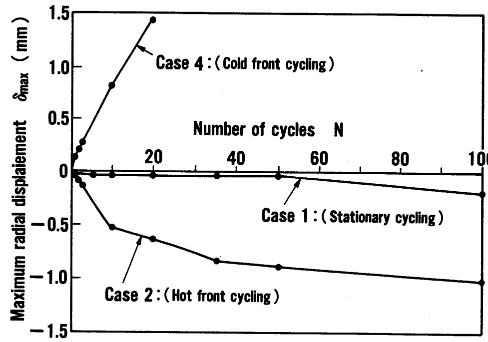

Fig.7 Ratcheting strain vs. number of cycles

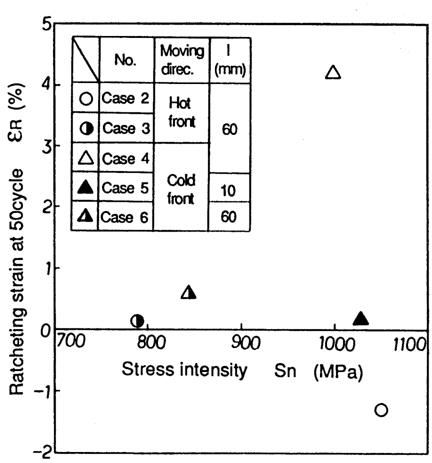

Fig.8 Ratcheting strain at 50 cycles vs. stress intensity Sn

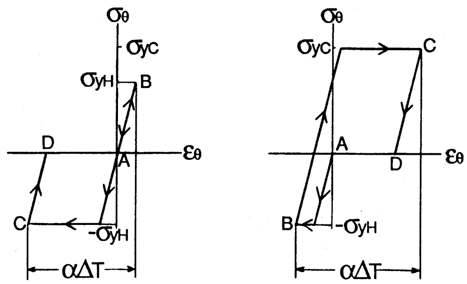

(a) Hot front (b) Cold front

Fig.9 Stress strain hysteresis loop of the step change

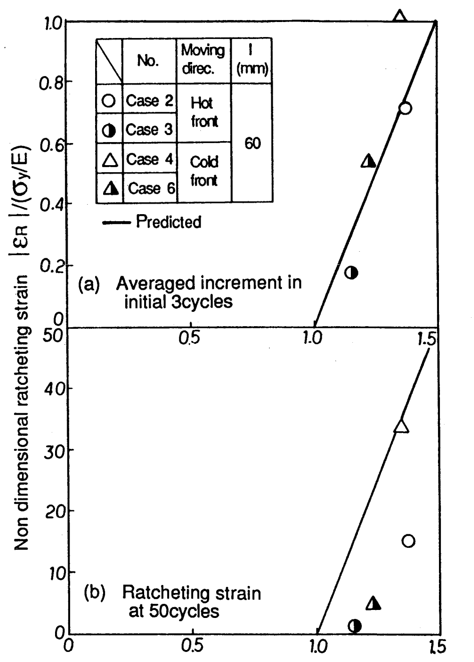

Fig.10 Comparison of predicted and experimental results